Correlation Effects on the Doped Triangular Lattice in View of the Physics of Sodium-Rich Na_xCoO_2

Frank Lechermann

I. Institut für Theoretische Physik, Universität Hamburg, D-20355 Hamburg, Germany

(Received 24 July 2008; published 27 January 2009)

The peculiar correlation effects on the triangular lattice are studied by means of the rotationally invariant slave boson method in a cellular cluster approach. Hence nonlocal correlations are included in a short-range regime. Their impact for the single-band Hubbard model is studied at half filling, i.e., on the Mott transition, and with doping. Using the realistic band structure of Na_xCoO_2, we may also shed light on the cobaltate physics for $x \geq 1/3$, with the in-plane transition from antiferromagnetic tendencies towards the onset of ferromagnetism for a finite Hubbard U.

DOI: 10.1103/PhysRevLett.102.046403 PACS numbers: 71.27.+a, 71.10.Fd, 71.30.+h, 75.30.Cr

The transition-metal oxide Na_xCoO_2, consisting of CoO_2 layers and Na ions in between, is one of the most fascinating examples of a doped correlated electron system on the triangular lattice. Albeit evidently the bare CoO_2 ($x = 0$) compound is metallic [1], surprisingly, the effect of strong correlation appears to be severe close to the band-insulating ($x = 1$) limit. Several experimental studies have revealed a rather rich phase diagram with highlighted physical properties such as superconductivity close to $x = 0.3$ (when intercalated with H_2O) [2], Pauli(Curie-Weiss)-like metallicity for $x < 0.5 (> 0.5)$ [3], in-plane antiferromagnetic (AFM) order at $x = 0.5$ [4], large thermopower around $0.71 < x < 0.84$ [5], charge disproportionation for $x > 0.5$ [6], and in-plane ferromagnetic (FM) order for $0.75 < x < 0.9$ [7,8]. Because of the sizable (t_{2g}, e_g) crystal-field (CF) splitting, the Co ion is expected to be in a low-spin state, with x controlling the residual occupation of the t_{2g} manifold. Hence Co^{4+} ($S = 1/2$) for $x = 0$ and Co^{3+} ($S = 0$) for $x = 1$. Yet the respective t_{2g} fillings and apparent Fermi surface (FS) for smaller x are still a matter of debate [9]. Though calculations based on the local density approximation (LDA) yield an t_{2g}-internal a_{1g}-e_g' CF splitting of -0.1 eV [10,11], only the a_{1g}-like bands are expected to be partially depleted for larger x. Those should form a single hexagonal FS sheet that is holelike; i.e., the hopping t within a nearest-neighbor (NN) tight-binding (TB) model is negative.

Concerning magnetism, LDA suggests FM order for already small x, although the AFM state is very close in energy [12,13]. Dynamical mean-field theory (DMFT) studies for the NN-TB Hubbard model on a triangular lattice [14,15] show an instability towards FM order only for $t > 0$. Gao *et al.* [16] described the appearance of a renormalized Stoner instability in an infinite-U Gutzwiller treatment of a third NN-TB model for Na_xCoO_2 (with the NN $t < 0$) at $x \sim 0.67$. Recently, a finite-U LDA + Gutzwiller approach obtained intralayer FM order at larger x [17], but contrary to experiment [1] finds full FM order at low doping. There are cluster approaches to the Hubbard model on the triangular lattice (e.g., [18,19]) but without incorporating the detailed electronic structure of Na_xCoO_2.

In the present work, realistic sodium cobaltate is investigated at larger Na doping, finite U, and by explicitly including NN correlation effects via the cellular cluster scheme. The puzzling change from AFM tendencies at small x towards the onset of intralayer FM order may be described within a Hubbard-like model using LDA dispersions and moderate U. The recently generalized rotationally invariant slave boson mean-field theory [20] (RISB) is applied to the problem [21], thereby tiling the lattice into NN triangles (see Fig. 1). To benchmark this approach in the present setup, we first studied the NN-TB single-band Hubbard model, written in the cellular cluster scheme as $H = H(\mathbf{K}) + H_\alpha$, i.e.,

$$H = \sum_{\mathbf{K}ij\sigma} \varepsilon^{\mathbf{K}}_{ij\sigma\sigma} c^\dagger_{\mathbf{K}i\sigma} c_{\mathbf{K}j\sigma} - t \sum_{\alpha ij\sigma} c^\dagger_{\alpha i\sigma} c_{\alpha j\sigma} + U \sum_{\alpha i} n_{\alpha i\uparrow} n_{\alpha i\downarrow}, \tag{1}$$

where α marks the cluster, ij are site indices on the cluster, σ denotes the spin ($\uparrow, \downarrow$), and $\mathbf{K}$ is the cluster wave vector. Note that for the cluster dispersion $\sum_{\mathbf{K}} \varepsilon^{\mathbf{K}}_{ij\sigma\sigma} = 0$ holds and the intracluster hopping is taken care of by the second term in (1). Within RISB the electron operator $c_{i\sigma}$ is represented as $\underline{c}_{i\sigma} = \hat{R}[\phi]^{\sigma\sigma'}_{ij} f_{j\sigma'}$, where R is a nondiagonal transformation operator that relates the physical operator to the

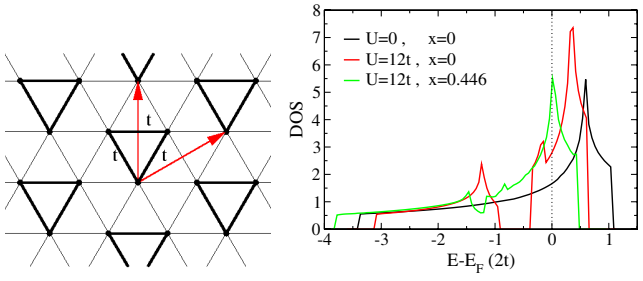

FIG. 1 (color online). 3-site cluster approach on the triangular lattice for isotropic NN hopping t. Left: lattice tiling, right: QP DOS for different interaction strength and doping.

quasiparticle (QP) operator $f_{i\sigma}$. The transformation $\hat{R}$ is written in terms of slave bosons $\{\phi_{An}\}$ with two indices, namely, A for the physical-electron state and n for the QP Fock state. It follows that the kinetic part of (1) is expressed via the QP operators with renormalized dispersions and the operator character of the local part is carried solely by the slave bosons [20]. Two constraints, namely, $\sum_{An}\phi^{\dagger}_{An}\phi_{An} = 1$ and $\sum_{Ann'}\phi^{\dagger}_{An'}\phi_{An}\langle n|f^{\dagger}_{i\sigma}f_{j\sigma'}|n'\rangle = f^{\dagger}_{i\sigma}f_{j\sigma'}$, to select the physical states are imposed through a set of Lagrange multipliers $\{\lambda\}$. A saddle-point solution is obtained by condensing the bosons and extremalizing the corresponding free energy $F(\{\phi\},\{\lambda\})$ [22]. The nonlocal QP weight matrix at saddle point reads $\mathbf{Z} = \mathbf{R}\mathbf{R}^{\dagger}$.

In the following, we study the paramagnetic (PM) phase where x denotes the electron doping normalized to a single orbital. The QP density of states (DOS) of the noninteracting model (bandwidth $W = 9t$), along with comparative interacting cases, is shown in Fig. 1. As displayed in Fig. 2, the RISB treatment for $x = 0$ reveals a first-order Mott transition at $U_c \sim 12.2t = 1.36W$, in agreement with values from exact diagonalization [23] ($\sim 12.1t$), cellular DMFT [18] ($\sim 10.5t$) and variational cluster approximation [19] ($\sim 12t$). Upon doping, the metallic state may be extended to larger U, although a breakdown of the conventional PM phase is found for small x at $U > U_c$. The magnitude of the off-diagonal QP weights Z_{ij} as well as of the NN spin correlation $\langle \mathbf{S}_i\mathbf{S}_j\rangle$ are enhanced close to the Mott transition. Note that $\langle \mathbf{S}_i\mathbf{S}_j\rangle$ is negative, i.e., of AFM character. Close to half filling, the Z_{ij} depend strongly on x and the onsite spin correlation is substantially enhanced for $U = 0$. The AFM strength of the intersite $\langle \mathbf{S}_i\mathbf{S}_j\rangle$ is decreasing with x, but remains slightly above the $U = 0$ case in the (meta)stability range of the PM phase. Note that the *global* FM instability was located around $x \sim 0.35$ [14].

For a realistic description of Na_xCoO_2 we first performed LDA calculations at different stoichiometries. A supercell involving the NN Co triangle of a given CoO_2 layer served as the base structure. Decorating the latter with additional Na ions *above* the Co sites yields the dopings $x = 0,\ 1/3,\ 2/3,\ 1$. No sodium ions above or below oxygen positions are considered, which should be adequate for the overall behavior with doping. A minimal model for the band structure is derived by representing the low-energy states by three maximally localized Wannier functions [24] (WFs) of a_{1g} type (see Fig. 3). Thus the full dispersions ($W \sim 1.2$ eV) are approximated through a downfolding procedure [25] via three a_{1g}-like bands.

Allowing for the essential behavior with x, a doping dependent Hamiltonian is obtained through a linear interpolation $H_{\mathrm{LDA}}(\mathbf{K}, x) = xH^{x_a}_{\mathrm{LDA}}(\mathbf{K}) + (1-x)H^{x_b}_{\mathrm{LDA}}(\mathbf{K})$, where x_a, x_b are the neighboring LDA-treated dopings. Note that the K points are generally on a three-dimensional (3D) mesh, describing the full band dispersions. In the full Hamiltonian (1) the kinetic term is now given by $H_{\mathrm{LDA}}(\mathbf{K}, x)$ *without* its on site (cluster) term t_{ij}. The latter replaces the model t in the "on site" quadratic term of (1), incorporating both the intersite hoppings on the Co cluster and the CF-terms on the individual ions. Be aware that the level of frustration is diminished via the symmetry-breaking Na occupations for intermediate x.

Contrary to the former model study, the realistic NN hoppings are now negative [14]. Their absolute value is more or less linearly decreasing with x, in average from 0.21 eV ($x = 0$) to 0.11 eV ($x = 1$). Any further explicit exchange couplings J are neglected. Integrating out the O states should render such couplings necessary [e.g., (A)FM exchange between the Co ions]. Yet a rigorous computation for metals is hard [13] and experiments revealed [8] that the values for a *pure* spin Hamiltonian are small. Calculations including Heisenberg-like terms in H resulted in no qualitative change for reasonable values of J (see footnote on the spin susceptibility). No long-range Coulomb potential is included; hence, explicit charge-disproportionated states do not appear (though site occupations surely differ). We concentrate the discussion on the

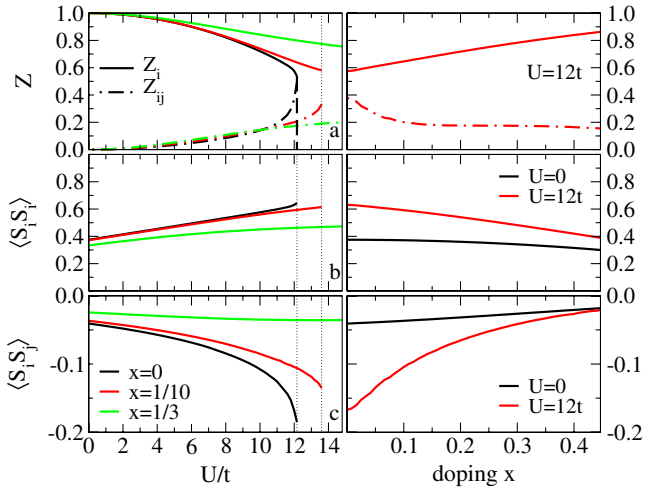

FIG. 2 (color online). Observables for the NN-TB Hubbard model ($t > 0$) on the triangular lattice. Left: U dependence for (a) QP weights, (b) on site spin correlation, and (c) NN spin correlation. Right: doping dependence of the same observables. The Z_{ij} are multiplied by 5 for better visibility.

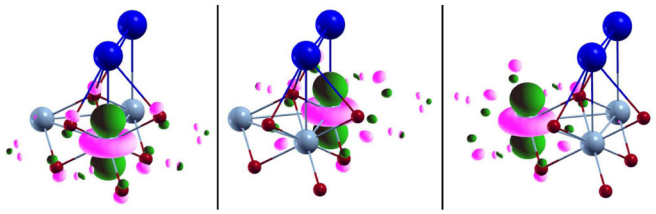

FIG. 3 (color online). From left to right: a_{1g}-like WFs in Na_xCoO_2 unit cell for $x = 2/3$ on Co(1), Co(2), and Co(3). Large blue (dark) balls denote Na ions, small red (gray) ball mark O ions.

phases for $x \geq 1/3$, since neglecting the remaining e_g' orbitals at small x may be improper. In fact, when performing the RISB calculation at $x = 0$, the Mott transition sets in at $U_c \sim 3.1$ eV. But this value is surely too small because of our orbital restrictions.

Figure 4 shows RISB results for $x = 1/3$, $2/3$ and with varying Na content for reasonable ranges/values of the interaction strength U. The resulting moderate size of the diagonal QP weight is in good agreement with experiment. Note that for $x = 1/3$ the offdiagonal Z_{ij} between sites on the triangle is positive with a maximum at $U \sim 3$ eV. For $x = 2/3$ its value is negative and still increasing in magnitude in the studied U range. The sign change implies that the hierachy in the correlation strength within the bonding-antibonding cluster orbitals is reversed. The on site spin correlations are saturating for large U, while the intersite $\langle \mathbf{S}_i \mathbf{S}_j \rangle$ are always negative but decrease in magnitude in the latter regime. For $x = 1/3$ the NN (spin) correlations are enhanced in magnitude between Co sites without Na on top. Because of CF effects, the orbital filling on a Co site tends generally to increase when placing Na on top. For the doping study, $U = 3$ eV and $U = 5$ eV were used. There the intersite Z_{ij} changes sign at $x \lesssim 0.5$ and has a minimum close to $x = 2/3$. As expected, the local spin correlations are strongly increased for finite U close to half filling [18]. The AFM character of the NN spin correlations is strengthened for intermediate x compared to the $U = 0$ case. However, interestingly, there is a crossover at $x \sim 2/3$ where the AFM magnitude for $U \neq 0$ becomes lower than in the latter case. Thus the AFM tendencies are suppressed by electronic correlations for large x, where the superexchange is diminished. This seems reminiscent of the Nagaoka mechanism [26] for the infinite-U Hubbard model on the square lattice, leading to FM order. But the Nagaoka state is not a ground state on the triangular lattice for a single hole [27].

To elucidate the problem of magnetic instabilities, a residual magnetic field $\mathbf{H}_f = \delta h \mathbf{e}_z$ is applied in the PM phase. Therefrom the uniform magnetic susceptibility is determined as $\chi \equiv \partial M / \partial H_f \approx \delta M / \delta h$, where δM is the residual magnetization induced by δh. Figure 5(a) shows the normalized response χ/χ_0, where χ_0 is the susceptibility for $U = 0$ [28]. It is seen that there is strong response for $x \sim 2/3$ and $U = 5$ eV, similar to results in the infinite-U limit [16]. Additionally, there is already a precursive regime for $x \gtrsim 0.62$ where FM ordering tendencies show up. This coincides with recent NMR measurements by Lang *et al.*, who find a crossover from AFM to FM correlations at $x = 0.63$–0.65 [29]. From the site- and component-resolved intersite spin correlations in the applied field, the dominant response of $\langle S_{iz} S_{jz} \rangle$ in the doping regime $0.62 \lesssim x \lesssim 0.7$ is again obvious. Note that also $U = 3$ eV exhibits minor FM ordering tendencies there. Interestingly, for $x \sim 0.35$ one may observe intralayer AFM response for both values of U. An AFM ordering signal is identified through locally favorable spin antialignment between Co(1)-Co(2) and Co(1)-Co(3), whereas Co (2)-Co(3) favor spin alignment. Remember that for $x = 1/3$ the Na ion is above Co(1); thus, the Co differentiation via neighboring Na ions obviously triggers the AFM tendencies. The outer-field induced AFM response is in line with the observation that such a field can lift the effects of

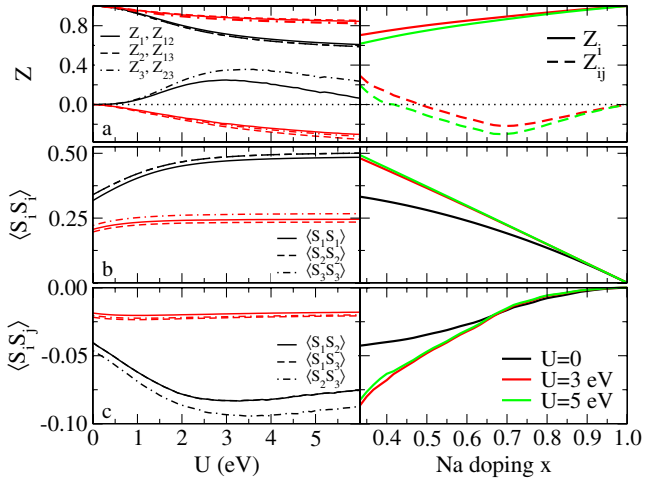

FIG. 4 (color online). Observables for Na_xCoO_2. Left: (a) site-resolved QP weights, (b) onsite- and (c) NN spin correlations for fixed doping. $x = 1/3$: (black/dark) lines, $x = 2/3$: (red/gray) lines. The offdiagonal Z_{ij} go to zero at $U = 0$. Co sites are numbered with Na filling: "1" has Na on top at $x = 1/3$, "2" also at $x = 2/3$. Right: doping dependence of the averaged observables. All Z_{ij} are multiplied by 50 for better visibility.

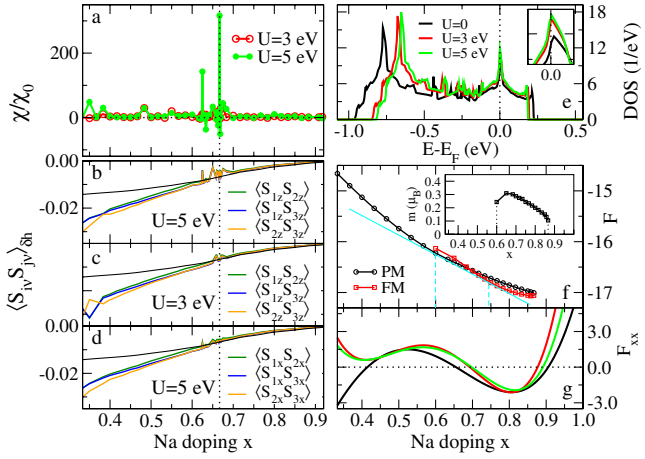

FIG. 5 (color online). Ordering tendencies and phase stability in Na_xCoO_2. (a) normalized magnetic susceptibility, (b)–(d) component-resolved NN spin correlation in the small field δh. Solid black line: $\langle S_{i\nu} S_{j\nu} \rangle_{\delta h}$ for $U = 0$. (e) QP DOS for $x = 2/3$. (f) RISB free energies for PM and FM phase of the single layer for $U = 5$ eV. Straight cyan (light gray) line: common tangent. Inset: net magnetic moment per Co ion in the FM phase. (g) Second derivative of the full PM free energy.

kinetic-energy frustration on a triangular cluster [30]. The fact that no clear long-range order is visible for larger x (i.e., negative χ/χ_0) may be explained by the present 3D model that cannot stabilize the A-type AFM phase (no proper interlayer resolution). Yet it is possible to stabilize FM order within a single layer by using only the 2D-projected LDA dispersion. Figure 5(f) shows the tieline construction between the PM and FM phase in this case. A stable *homogeneous* FM order is revealed for $x \gtrsim 0.74$, with magnetic moments close to experimental values. The onset of the *heterogeneous* phase at $x \sim 0.6$ matches the begin of FM tendencies in the full 3D model. In this context, hints for a spin-liquid ground state at $0.71 \leq x < 0.75$ [31] are rather interesting. Either 2D phase becomes hard to stabilize numerically for $x \gtrsim 0.87$.

Though at $x = 2/3$ the Fermi level is located in the upper maximum peak of the QP DOS [see Fig. 5(e)], our study reveals that a Stoner instability cannot be the sole origin for magnetic ordering. The nonmonotonic behavior of Z_{ij}, the subtle change of the frustration level with x, the precursive FM regime, the PM-FM phase competition as well as the breakdown of the 2D phases at very large doping are all pointing towards nonlocal correlations as an additional important ingredient. As a side effect, plotting $\partial^2 F/\partial x^2$ [Fig. 5(g)] shows that the present 3D-PM phase becomes unstable with respect to doping for $x \gtrsim 0.7$, while U stabilizes the phase for $x < 0.5$. Phase separation is experimentally indeed observed at large x (e.g., [32] and references therein).

In conclusion, it was shown that the RISB formalism may describe the essential physics of the NN-TB Hubbard model on the triangular lattice, including the first-order Mott transition and the Fermi-liquid upon doping. The magnetic behavior with doping in Na_xCoO_2 can be understood with a cluster Hubbard model using LDA dispersions. In very good quantitative agreement with experimental data, the change from AFM to FM tendencies with a final first-order transition in x into an in-plane FM phase was revealed. For the correlated physics with intralayer FM tendencies starting at $x \gtrsim 0.62$ and 2D-FM order for $0.74 < x < 0.87$, an interaction strength $U > 3$ eV is sufficient. Since then $U/W \gtrsim 2.5$ and the strongly correlated regime is already reached, without implying that $x = 0$ is Mott insulating (due to the probably increased orbital fluctuations there). Further studies, also at small doping, including long-range and interlayer correlations are needed to clarify more details.

The author is indebted to M. Potthoff, I. I. Mazin, and P. S. Cornaglia for helpful discussions. This work was supported by the SFB 668.

[1] C. de Vaulx, M.-H. Julien, and C. Berthier *et al.*, Phys. Rev. Lett. **98**, 246402 (2007).
[2] K. Takada, H. Sakurai, and E. Takayama-Muromachi *et al.*, Nature (London) **422**, 53 (2003).
[3] M. L. Foo, Y. Wang, and S. Watauchi *et al.*, Phys. Rev. Lett. **92**, 247001 (2004).
[4] P. Mendels, D. Bono, and J. Bobroff *et al.*, Phys. Rev. Lett. **94**, 136403 (2005).
[5] Y. Wang, N. S. Rogado, R. J. Cava, and N. P. Ong, Nature (London) **423**, 425 (2003).
[6] I. R. Mukhamedshin, H. Alloul, G. Collin, and N. Blanchard, Phys. Rev. Lett. **94**, 247602 (2005).
[7] A. T. Boothroyd, R. Coldea, and D. A. Tennant *et al.*, Phys. Rev. Lett. **92**, 197201 (2004).
[8] S. P. Bayrakci, I. Mirebeau, and P. Bourges *et al.*, Phys. Rev. Lett. **94**, 157205 (2005).
[9] C. A. Marianetti and G. Kotliar, Phys. Rev. Lett. **98**, 176405 (2007).
[10] F. Lechermann, S. Biermann, and A. Georges, Prog. Theor. Phys. Suppl. **160**, 233 (2005).
[11] D. Pillay, M. D. Johannes, I. I. Mazin, and O. K. Andersen, Phys. Rev. B **78**, 012501 (2008).
[12] D. Singh, Phys. Rev. B **61**, 13 397 (2000).
[13] M. D. Johannes, I. I. Mazin, and D. J. Singh, Phys. Rev. B **71**, 214410 (2005).
[14] J. Merino, B. J. Powell, and R. H. McKenzie, Phys. Rev. B **73**, 235107 (2006).
[15] K. Aryanpour, W. E. Pickett, and R. T. Scalettar, Phys. Rev. B **74**, 085117 (2006).
[16] M. Gao, S. Zhou, and Z. Wang, Phys. Rev. B **76**, 180402 (2007).
[17] G.-T. Wang, X. Dai, and Z. Fang, Phys. Rev. Lett. **101**, 066403 (2008).
[18] B. Kyung, Phys. Rev. B **75**, 033102 (2007).
[19] P. Sahebsara and D. Sénéchal, Phys. Rev. Lett. **100**, 136402 (2008).
[20] F. Lechermann, A. Georges, G. Kotliar, and O. Parcollet, Phys. Rev. B **76**, 155102 (2007).
[21] A different slave spin cluster mean-field theory was presented recently in a similar context by S. R. Hassan and L. de' Medici, arXiv:0805.3550.
[22] Gaussian smearing of $\sim$1 meV is used for the K-point integration, introducing a small effective temperature.
[23] M. Capone, L. Capriotti, F. Becca, and S. Caprara, Phys. Rev. B **63**, 085104 (2001).
[24] N. Marzari and D. Vanderbilt, Phys. Rev. B **56**, 12847 (1997).
[25] I. Souza, N. Marzari, and D. Vanderbilt, Phys. Rev. B **65**, 035109 (2001).
[26] Y. Nagaoka, Phys. Rev. **147**, 392 (1966).
[27] J. O. Haerter and B. S. Shastry, Phys. Rev. Lett. **95**, 087202 (2005).
[28] A magnetic response of the cobaltate model for $U = 0$ may surely be achieved via an explicit exchange term.
[29] G. Lang, J. Bobroff, H. Alloul, G. Collin, and N. Blanchard, Phys. Rev. B **78**, 155116 (2008).
[30] W. Barford and J. H. Kim, Phys. Rev. B **43**, 559 (1991).
[31] L. Balicas, Y. J. Jo, G. J. Shu, F. C. Chou, and P. A. Lee, Phys. Rev. Lett. **100**, 126405 (2008).
[32] M. Lee, L. Viciu, and L. Li *et al.*, Nature Mater. **5**, 537 (2006).